Published September 16, 2013

Wang, L., S.J. Li, A. Sidhu, L. Zhu, Y. Liang, R.B. Freedman, and C.C. Wang. 2009. Reconstitution of human Ero1-Lalpha/protein-disulfide isomerase oxidative folding pathway in vitro. Position-dependent differences in role between the a and a' domains of protein-disulfide isomerase. *J. Biol. Chem.* 284:199–206. http://dx.doi.org/10.1074/jbc.M806645200

Zhang, K., and R.J. Kaufman. 2008. From endoplasmic-reticulum stress to the inflammatory response. *Nature*. 454:455–462. http://dx.doi.org/10.1038/nature07203

Zhou, Y., T. Cierpicki, R.H. Jimenez, S.M. Lukasik, J.F. Ellena, D.S. Cafiso, H. Kadokura, J. Beckwith, and J.H. Bushweller. 2008. NMR solution structure of the integral membrane enzyme DsbB: functional insights into DsbB-catalyzed disulfide bond formation. *Mol. Cell.* 31:896–908. http://dx.doi.org/10.1016/j.molcel.2008.08.028

Zito, E., E.P. Melo, Y. Yang, A. Wahlander, T.A. Neubert, and D. Ron. 2010. Oxidative protein folding by an endoplasmic reticulum-localized peroxiredoxin. *Mol. Cell.* 40:787–797. http://dx.doi.org/10.1016/j.molcel.2010.11.010

Araki et al., http://www.jcb.org/cgi/content/full/jcb.201303027/DC1

A

Gene_Symbol	Identified Number	Protein Name	1	2	3	4	5	6	7	8
Bait protein	Total 8 trials									
Ero1α	8	ERO1-like	9	10	10	10	10	9	9	5
Ero1α or Ero1β	8	ERO1-like or ERO1-like β	2	2	2	2	2	2	2	2
HIT Preys										
PDI (P4HB)	8	prolyl 4-hydroxylase, β subunit	19	19	19	21	19	20	22	15
ERp57 (PDIA3)	8	protein disulfide isomerase A3	7	7	7	5	7	7	6	4
ERp72 (PDIA4)	8	protein disulfide isomerase A4	2	3	4	2	1	1	3	3
P5 (PDIA6)	8	protein disulfide isomerase A6	7	6	6	7	7	7	7	5
ERp46 (TXNDC5)	8	thioredoxin domain containing 5	2	2	3	2	2	2	2	2
CANX	8	calnexin	4	4	5	4	1	1	2	2
ERp44 (TXNDC4)	7	thioredoxin domain containing 4 (endoplasmic reticulum)	6	5	6	6	5	5	5	0
EVIS1	6	ecotropic viral integration site 5-like; isoform 2	0	1	0	1	1	1	1	1
SCYL2	6	SCY1-like 2 protein	21	20	19	18	0	0	2	3
CALR	4	calreticulin	4	3	3	2	0	0	0	0
ERdj5 (DNAJC10)	4	DnaJ (Hsp40) homolog, subfamily C, member 10	4	5	3	2	0	0	0	0
PRDX4	4	peroxiredoxin 4	0	0	0	0	1	1	1	1
UGCGL1	4	UDP-glucose ceramide glucosyltransferase-like 1; isoform 2	7	5	6	3	0	0	0	0
Total Hit preys	13		16	15	15	14	8	8	12	14

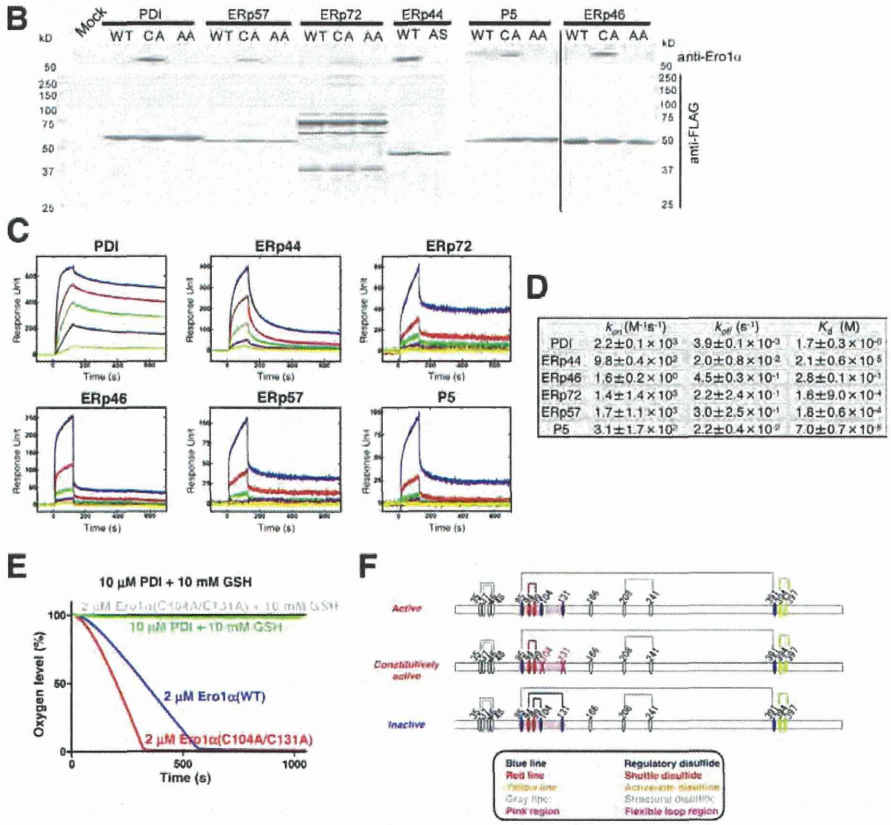

	k_{on} ($M^{-1}s^{-1}$)	k_{off} (s^{-1})	K_d (M)
PDI	$2.2\pm0.1\times10^{3}$	$3.9\pm0.1\times10^{-3}$	$1.7\pm0.3\times10^{-6}$
ERp44	$9.8\pm0.4\times10^{2}$	$2.0\pm0.8\times10^{-2}$	$2.1\pm0.6\times10^{-5}$
ERp46	$1.6\pm0.2\times10^{0}$	$4.5\pm0.3\times10^{-1}$	$2.8\pm0.1\times10^{-1}$
ERp72	$1.4\pm1.4\times10^{3}$	$2.2\pm2.4\times10^{-1}$	$1.6\pm9.0\times10^{-4}$
ERp57	$1.7\pm1.1\times10^{3}$	$3.0\pm2.5\times10^{-1}$	$1.8\pm0.6\times10^{-4}$
P5	$3.1\pm1.7\times10^{2}$	$2.2\pm0.4\times10^{-2}$	$7.0\pm0.7\times10^{-5}$

Figure S1. **Ero1-α binds to ER-resident oxidoreductases.** (A) Ero1-α(WT)–FLAG was expressed in HEK293T cells, and anti-FLAG immunoprecipitates were analyzed by direct nanoflow liquid chromatography/tandem mass spectrometry. Preys identified during eight independent trials are listed. Each number indicates the identified peptide number of each protein in individual experiments. Gray bars show the poor reproducible preys or nonoxidoreductases. (B) HEK293T cells were transfected with a series of oxidoreductases, including the wild type (WT) and their mutants (CA and AA), as indicated. Cell lysates were immunoprecipitated by anti-FLAG antibody, subjected to SDS-PAGE on two separate membranes, and analyzed by immunoblotting with anti–Ero1-α (top) and anti-FLAG (bottom) antibodies. A black line on the right indicates the removal of intervening lanes from one of the membranes for presentation purposes. Note that ERp44 contains a CRFS motif in its active site, and its mutant is ARFS (AS). (C) Recombinant Ero1-α(WT) proteins were immobilized on the surface of a sensor chip. Binding responses were collected at five different concentrations (0.444–36 μM, in a threefold dilution series) of oxidoreductases under redox conditions equivalent to those in the ER (GSH/GSSG ratio = 4:1). Association or dissociation rate constants (k_{on} or k_{off}) were determined using a two-state reaction model. (D) SPR-quantified result. Data represent means ± SE from at least three individual experiments. (E) Assays were conducted in a sealed chamber starting with air-saturated buffer containing 10 mM GSH, which was regarded as the 100% oxygen level (~250 μM oxygen). Control samples contained 2 μM Ero1-α(WT) or 10 μM PDI in the presence of 10 mM GSH. Oxidation of reduced PDI was initiated by the injection of 2 μM Ero1-α or Ero1-α(C104A/C131A) and was monitored with an oxygen electrode. (F) Schematic and representative diagrams of the active (O_{x1}) and inactive (O_{x2}) forms of Ero1-α and its constitutively active mutant Ero1-α(C104A/C131A).

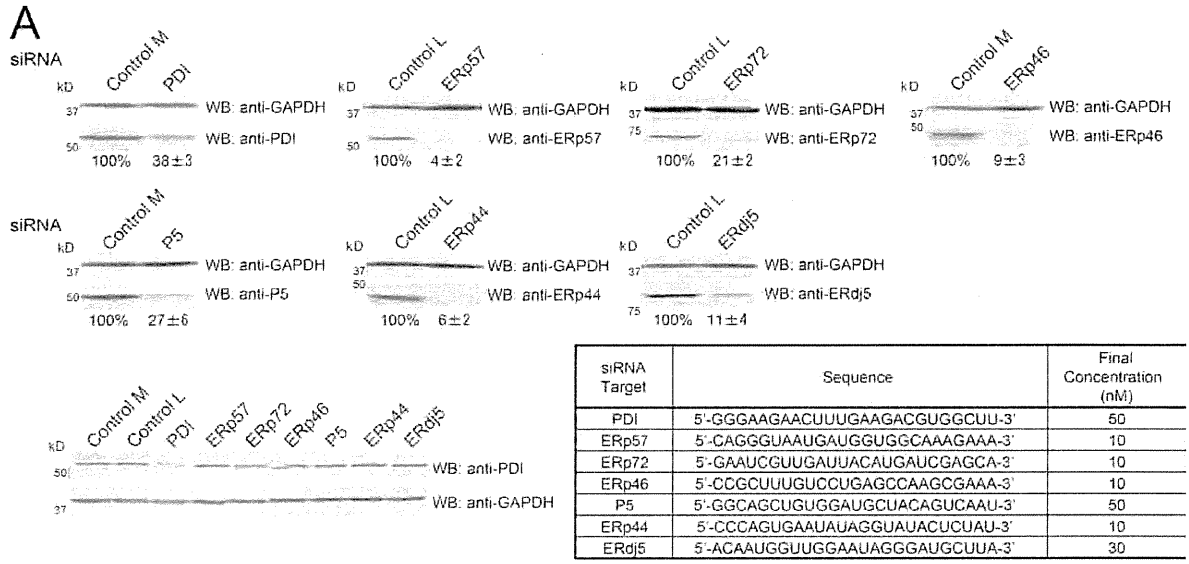

siRNA Target	Sequence	Final Concentration (nM)
PDI	5'-GGGAAGAACUUUGAAGACGUGGCUU-3'	50
ERp57	5'-CAGGGUAAUGAUGGUGGCAAAGAAA-3'	10
ERp72	5'-GAAUCGUUGAUUACAUGAUCGAGCA-3'	10
ERp46	5'-CCGCUUUGUCCUGAGCCAAGCGAAA-3'	10
P5	5'-GGCAGCUGUGGAUGCUACAGUCAAU-3'	50
ERp44	5'-CCCAGUGAAUAUAGGUAUACUCUAU-3'	10
ERdj5	5'-ACAAUGGUUGGAAUAGGGAUGCUUA-3'	30

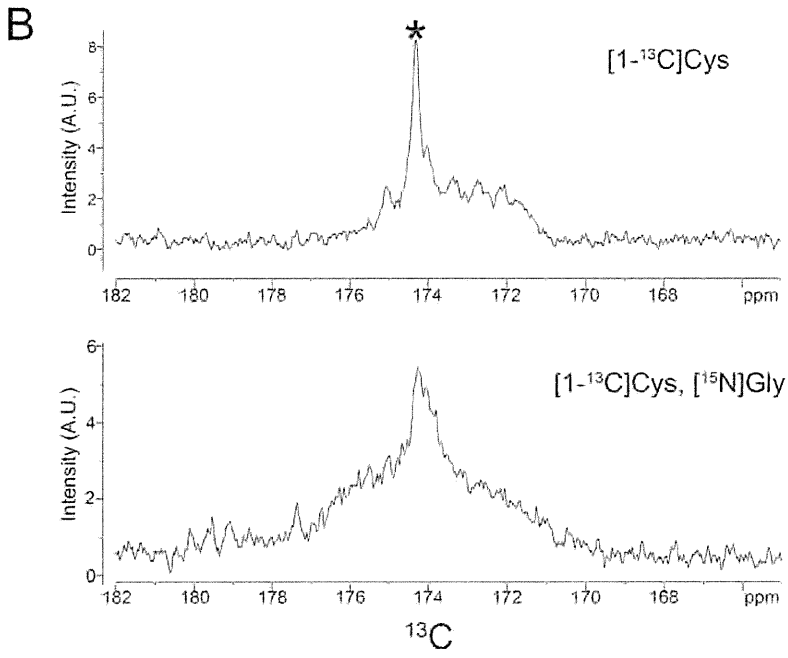

Figure S2. **Validation of siRNA silencing and annotation of Cys94 with a double-labeling method.** (A) siRNA-mediated silencing in HEK293T cells was achieved via transfection of predesigned siRNAs. The sequences and concentrations are summarized in the bottom table. As controls, two different siRNAs (L, low GC content; M, medium GC content) were used, depending on the GC content of each siRNA. At 72 h after transfection, cell lysates were analyzed by SDS-PAGE and immunoblotted against the target protein and GAPDH. Endogenous expression levels of PDI under each siRNA silencing condition were detected as controls and are shown in the bottom row in A. Numbers below indicate knockdown efficiency. (B) ^{13}C NMR spectra of constitutively active Ero1-α, which was selectively labeled with ^{13}C at the carbonyl carbons of cysteine residues ([1-^{13}C]Cys; top) or both at [1-^{13}C]Cys and at the nitrogen of glycine residues ([^{15}N]Gly; bottom). The spectrum of the unlabeled protein has been subtracted. The asterisk indicates the peak originating from Cys94, which was significantly reduced after selective double labeling as a result of rapid transverse nuclear spin relaxation (Serve et al., 2010). WB, Western blot; A.U., arbitrary unit.

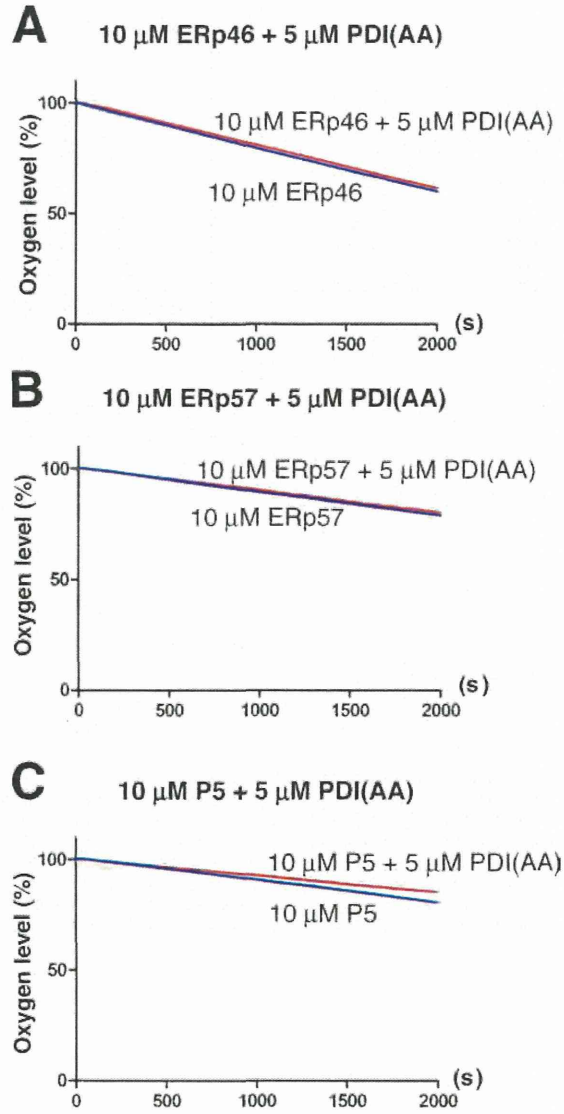

Figure S3. **PDI(AA) does not accelerate the Ero1-α oxidation system.** (A–C) Oxygen consumption was assayed in the presence of 10 mM GSH and 10 μM ERp46 (A), ERp57 (B), and P5 (C) either with or without 5 μM PDI(AA).

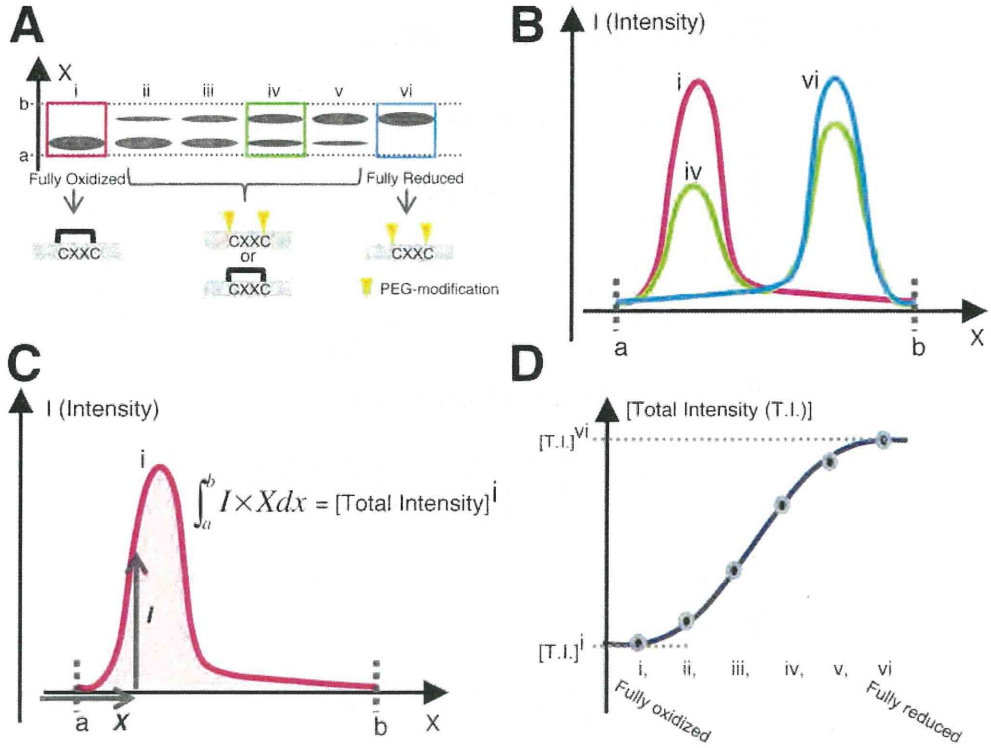

Figure S4. **Method used to calculate the K_{eq} values.** The following procedure was used to calculate the K_{eq} values from SDS-PAGE bands. To simplify the model, the redox protein containing one active domain is shown. (A) Free sulfhydryl groups on the cysteine residues were modified with mPEG2000-mal (molecular weight of 2,000) after incubation with different $[GSH]^2/[GSSG]$ ratios in a buffer containing GSSG and varying concentrations of GSH followed by SDS-PAGE and CBB staining. The active sites of the reduced form (vi, blue column) were modified with mPEG2000-mal. As a result, the reduced form migrated more slowly than the oxidized form. After CBB staining, the mean intensity of the horizontal pixels in each box was calculated along a line from the lower side of the fully oxidized form a to the upper side of the fully reduced form b using ImageJ (National Institutes of Health). (B) The x axis represents the longitudinal axis in A, and the y axis is the calculated mean pixel intensity. Total intensities were calculated using the integration shown in C. (D) For fitting, the values for the completely oxidized ($[T.I]^i$) or reduced state ($[T.I]^{vi}$) were regarded as 0 or 1, respectively, and all intermediate states were recalibrated as shown in Fig. 6 B.

Table S1. **List of publications reporting Ero1-α–related assays and having a bearing on this study**

Ero1-α–related assay	Figure in this study	Studies related to this study						Other studies
		PDI	ERp44	ERp57	ERp46	P5	ERp72	
Immunoprecipitation of Ero1-α (detecting WT oxidoreductase)	1 A, 6 A, and S1 A	Benham et al., 2000; Mezghrani et al., 2001; Anelli et al., 2002; Bertoli et al., 2004; Otsu et al., 2006; Appenzeller-Herzog et al., 2008, 2010; Masui et al., 2011; Benham et al., 2013	Anelli et al., 2002, 2003; Bertoli et al., 2004; Otsu et al., 2006	Appenzeller-Herzog et al., 2010			Appenzeller-Herzog et al., 2010	
Immunoprecipitation of the CXXA/AXXA mutant of oxidoreductase (detecting Ero1-α)	S1 B and 6 A	Jessop et al., 2009b; Schulman et al., 2010; Zito et al., 2010		Jessop et al., 2007, 2009a,b; Schulman et al., 2010	Jessop et al., 2009b	Jessop et al., 2009b; Schulman et al., 2010	Schulman et al., 2010	ERp18: Jessop et al., 2009b; ERp18, TMX, PDIR, and PDIp: Schulman et al., 2010
Activation of Ero1-α by oxidoreductase (e.g., detecting the $O_{x1}/(O_{x1} + O_{x2})$ ratio)	2, A and B	Otsu et al., 2006[a]; Appenzeller-Herzog et al., 2008	Otsu et al., 2006[a]	Appenzeller-Herzog et al., 2008				TMX3: Appenzeller-Herzog et al., 2008
In vitro oxidase assays (e.g., oxygen consumption assay and RNase assay)	1, D and E; and S1 E	Tsai and Rapoport, 2002; Baker et al., 2008; Wang et al., 2009; Chambers et al., 2010; Inaba et al., 2010; Zito et al., 2010; Araki and Nagata, 2011a; Masui et al., 2011; Wang et al., 2011	Not analyzed in this study[b]	Inaba et al., 2010				
In vitro binding assays (e.g., SPR assay and ITC measurements)	1 B and S1, C and D	Wang et al., 2009; Inaba et al., 2010; Araki and Nagata, 2011a; Masui et al., 2011	Masui et al., 2011	Inaba et al., 2010				

ITC, isothermal titration calorimetry.
[a]Otsu et al. (2006) examined the redox states of Ero1-α when PDI or ERp44 was overexpressed. However, at that time, the redox states of Ero1-α were unknown to correlate with its activation.
[b]Because ERp44 has a CRFS motif, it has no detectable redox activity. Hence, it was not listed under the oxygen consumption assay.

References

Anelli, T., M. Alessio, A. Mezghrani, T. Simmen, F. Talamo, A. Bachi, and R. Sitia. 2002. ERp44, a novel endoplasmic reticulum folding assistant of the thioredoxin family. *EMBO J.* 21:835–844. http://dx.doi.org/10.1093/emboj/21.4.835

Anelli, T., M. Alessio, A. Bachi, L. Bergamelli, G. Bertoli, S. Camerini, A. Mezghrani, E. Ruffato, T. Simmen, and R. Sitia. 2003. Thiol-mediated protein retention in the endoplasmic reticulum: the role of ERp44. *EMBO J.* 22:5015–5022. http://dx.doi.org/10.1093/emboj/cdg491

Appenzeller-Herzog, C., J. Riemer, B. Christensen, E.S. Sørensen, and L. Ellgaard. 2008. A novel disulphide switch mechanism in Ero1alpha balances ER oxidation in human cells. *EMBO J.* 27:2977–2987. http://dx.doi.org/10.1038/emboj.2008.202

Appenzeller-Herzog, C., J. Riemer, E. Zito, K.T. Chin, D. Ron, M. Spiess, and L. Ellgaard. 2010. Disulphide production by Ero1α-PDI relay is rapid and effectively regulated. *EMBO J.* 29:3318–3329. http://dx.doi.org/10.1038/emboj.2010.203

Araki, K., and K. Nagata. 2011a. Functional in vitro analysis of the ERO1 protein and protein-disulfide isomerase pathway. *J. Biol. Chem.* 286:32705–32712. http://dx.doi.org/10.1074/jbc.M111.227181

Baker, K.M., S. Chakravarthi, K.P. Langton, A.M. Sheppard, H. Lu, and N.J. Bulleid. 2008. Low reduction potential of Ero1alpha regulatory disulphides ensures tight control of substrate oxidation. *EMBO J.* 27:2988–2997. http://dx.doi.org/10.1038/emboj.2008.230

Benham, A.M., A. Cabibbo, A. Fassio, N. Bulleid, R. Sitia, and I. Braakman. 2000. The CXXCXXC motif determines the folding, structure and stability of human Ero1-Lalpha. *EMBO J.* 19:4493–4502. http://dx.doi.org/10.1093/emboj/19.17.4493

Benham, A.M., M. van Lith, R. Sitia, and I. Braakman. 2013. Ero1-PDI interactions, the response to redox flux and the implications for disulfide bond formation in the mammalian endoplasmic reticulum. *Philos. Trans. R. Soc. Lond. B Biol. Sci.* 368:20110403. http://dx.doi.org/10.1098/rstb.2011.0403

Bertoli, G., T. Simmen, T. Anelli, S.N. Molteni, R. Fesce, and R. Sitia. 2004. Two conserved cysteine triads in human Ero1alpha cooperate for efficient disulfide bond formation in the endoplasmic reticulum. *J. Biol. Chem.* 279:30047–30052. http://dx.doi.org/10.1074/jbc.M403192200

Chambers, J.E., T.J. Tavender, O.B. Oka, S. Warwood, D. Knight, and N.J. Bulleid. 2010. The reduction potential of the active site disulfides of human protein disulfide isomerase limits oxidation of the enzyme by Ero1α. *J. Biol. Chem.* 285:29200–29207. http://dx.doi.org/10.1074/jbc.M110.156596

Inaba, K., S. Masui, H. Iida, S. Vavassori, R. Sitia, and M. Suzuki. 2010. Crystal structures of human Ero1α reveal the mechanisms of regulated and targeted oxidation of PDI. *EMBO J.* 29:3330–3343. http://dx.doi.org/10.1038/emboj.2010.222

Jessop, C.E., S. Chakravarthi, N. Garbi, G.J. Hämmerling, S. Lovell, and N.J. Bulleid. 2007. ERp57 is essential for efficient folding of glycoproteins sharing common structural domains. *EMBO J.* 26:28–40. http://dx.doi.org/10.1038/sj.emboj.7601505

Jessop, C.E., T.J. Tavender, R.H. Watkins, J.E. Chambers, and N.J. Bulleid. 2009a. Substrate specificity of the oxidoreductase ERp57 is determined primarily by its interaction with calnexin and calreticulin. *J. Biol. Chem.* 284:2194–2202. http://dx.doi.org/10.1074/jbc.M808054200

Jessop, C.E., R.H. Watkins, J.J. Simmons, M. Tasab, and N.J. Bulleid. 2009b. Protein disulphide isomerase family members show distinct substrate specificity: P5 is targeted to BiP client proteins. *J. Cell Sci.* 122:4287–4295. http://dx.doi.org/10.1242/jcs.059154

Masui, S., S. Vavassori, C. Fagioli, R. Sitia, and K. Inaba. 2011. Molecular bases of cyclic and specific disulfide interchange between human ERO1alpha protein and protein-disulfide isomerase (PDI). *J. Biol. Chem.* 286:16261–16271. http://dx.doi.org/10.1074/jbc.M111.231357

Mezghrani, A., A. Fassio, A. Benham, T. Simmen, I. Braakman, and R. Sitia. 2001. Manipulation of oxidative protein folding and PDI redox state in mammalian cells. *EMBO J.* 20:6288–6296. http://dx.doi.org/10.1093/emboj/20.22.6288

Otsu, M., G. Bertoli, C. Fagioli, E. Guerini-Rocco, S. Nerini-Molteni, E. Ruffato, and R. Sitia. 2006. Dynamic retention of Ero1alpha and Ero1beta in the endoplasmic reticulum by interactions with PDI and ERp44. *Antioxid. Redox Signal.* 8:274–282. http://dx.doi.org/10.1089/ars.2006.8.274

Schulman, S., B. Wang, W. Li, and T.A. Rapoport. 2010. Vitamin K epoxide reductase prefers ER membrane-anchored thioredoxin-like redox partners. *Proc. Natl. Acad. Sci. USA.* 107:15027–15032. http://dx.doi.org/10.1073/pnas.1009972107

Serve, O., Y. Kamiya, A. Maeno, M. Nakano, C. Murakami, H. Sasakawa, Y. Yamaguchi, T. Harada, E. Kurimoto, M. Yagi-Utsumi, et al. 2010. Redox-dependent domain rearrangement of protein disulfide isomerase coupled with exposure of its substrate-binding hydrophobic surface. *J. Mol. Biol.* 396:361–374. http://dx.doi.org/10.1016/j.jmb.2009.11.049

Tsai, B., and T.A. Rapoport. 2002. Unfolded cholera toxin is transferred to the ER membrane and released from protein disulfide isomerase upon oxidation by Ero1. *J. Cell Biol.* 159:207–216. http://dx.doi.org/10.1083/jcb.200207120

Wang, L., S.J. Li, A. Sidhu, L. Zhu, Y. Liang, R.B. Freedman, and C.C. Wang. 2009. Reconstitution of human Ero1-Lalpha/protein-disulfide isomerase oxidative folding pathway in vitro. Position-dependent differences in role between the a and a' domains of protein-disulfide isomerase. *J. Biol. Chem.* 284:199–206. http://dx.doi.org/10.1074/jbc.M806645200

Wang, L., L. Zhu, and C.C. Wang. 2011. The endoplasmic reticulum sulfhydryl oxidase Ero1β drives efficient oxidative protein folding with loose regulation. *Biochem. J.* 434:113–121. http://dx.doi.org/10.1042/BJ20101357

Zito, E., E.P. Melo, Y. Yang, A. Wahlander, T.A. Neubert, and D. Ron. 2010. Oxidative protein folding by an endoplasmic reticulum-localized peroxiredoxin. *Mol. Cell.* 40:787–797. http://dx.doi.org/10.1016/j.molcel.2010.11.010

⌘ *Author's Choice*

THE JOURNAL OF BIOLOGICAL CHEMISTRY VOL. 288, NO. 41, pp. 29586–29594, October 11, 2013

Dynamic Regulation of Ero1α and Peroxiredoxin 4 Localization in the Secretory Pathway*[S]

Received for publication, March 8, 2013, and in revised form, August 23, 2013 Published, JBC Papers in Press, August 26, 2013, DOI 10.1074/jbc.M113.467845

Taichi Kakihana[‡§1], **Kazutaka Araki**[¶1], **Stefano Vavassori**[‖], **Shun-ichiro Iemura**[**], **Margherita Cortini**[‖], **Claudio Fagioli**[‖], **Tohru Natsume**[¶], **Roberto Sitia**[‖2,3], **and Kazuhiro Nagata**[§2,4]

From the [‡]*Department of Molecular and Cellular Biology, Institute for Frontier Medical Sciences, Kyoto University, 53 Kawahara-cho, Shogoin, Sakyo-ku, Kyoto 606-8397, Japan, the* [§]*Laboratory of Molecular and Cellular Biology, Faculty of Life Sciences, Kyoto Sangyo University, Motoyama, Kamigamo, Kita-ku, Kyoto 603-8555, Japan, the* [‖]*Università Vita-Salute San Raffaele Scientific Institute, Division of Genetics and Cell Biology, Via Olgettina 58, I-20132 Milan, Italy, the* [¶]*Molecular Profiling Research Center for Drug Discovery, National Institute of Advanced Industrial Science and Technology, 2-4-7 Aomi, Koto-ku, Tokyo 135-0064, Japan, and the* [**]*Medical Industry Translational Research Center, Fukushima Medical University, 1 Hikarigaoka, Fukushima 960-1295, Japan*

Background: Ero1α and peroxiredoxin 4 contribute to disulfide formation in the early secretory compartment (ESC), but lack known retention signals.
Results: Retention and localization of Ero1α and peroxiredoxin 4 are maintained through multistep and pH-dependent interactions with PDI and ERp44 in ESC.
Conclusion: PDI and ERp44 dynamically localize Ero1α and peroxiredoxin 4 in ESC.
Significance: The levels and localization of four interactors allow differential ESC redox control.

In the early secretory compartment (ESC), a network of chaperones and enzymes assists oxidative folding of nascent proteins. Ero1 flavoproteins oxidize protein disulfide isomerase (PDI), generating H_2O_2 as a byproduct. Peroxiredoxin 4 (Prx4) can utilize luminal H_2O_2 to oxidize PDI, thus favoring oxidative folding while limiting oxidative stress. Interestingly, neither ER oxidase contains known ER retention signal(s), raising the question of how cells prevent their secretion. Here we show that the two proteins share similar intracellular localization mechanisms. Their secretion is prevented by sequential interactions with PDI and ERp44, two resident proteins of the ESC-bearing KDEL-like motifs. PDI binds preferentially Ero1α, whereas ERp44 equally retains Ero1α and Prx4. The different binding properties of Ero1α and Prx4 increase the robustness of ER redox homeostasis.

Secretory or membrane proteins attain their native state in the ER,[5] under the assistance of a vast array of resident chaperones and enzymes. Formation, cleavage, or rearrangement of disulfide bond is catalyzed by oxidoreductases of the protein disulfide isomerase (PDI) family, which in humans lists over 20 members (1). The *CXXC* motifs in thioredoxin-like active domains, so-called a-domains, mediate disulfide interchange reactions. Redox-inactive domains, or b-domains, of similar structure but lacking *CXXC* motifs are frequently found in PDI family members. In PDI, for instance, the two redox-active domains (a- and a′-domain) are separated by the b- and b′-domains (a-b-b′-a′). The b′-domain provides a hydrophobic pocket onto which client proteins and ER oxidoreductin-1 (Ero1) molecules dock (2, 3).

ERp44 has an a-b-b′ domain organization (4) and plays important roles in the early secretory compartment (ESC) (5). Unlike PDI and other KDEL-bearing proteins, ERp44 accumulates in the ER-Golgi intermediate compartment (ERGIC) and cis Golgi (6, 7). In its a-domain, ERp44 has a conserved redox motif, CRFS, whose cysteine (Cys-29) is used to form mixed disulfides with IgM, adiponectin, and other client proteins for thiol-dependent quality control (8–10). ERp44 binds and regulates Ero1α and β, two key ESC-resident oxidases (11), and displays pH-dependent conformational change in ESC to prominently retrieve Ero1 and premature secretory proteins from the ERGIC to the ER (12).

Upon transferring disulfide bonds to incoming client proteins, PDI can be efficiently reoxidized by members of the Ero1 family (Ero1α and Ero1β in mammals). As these flavoproteins use oxygen as an electron acceptor generating hydrogen peroxide as a byproduct, the question arose as to how professional secretory cells could fold abundant proteins rich in disulfide bonds with limiting oxidative stress. A solution of this paradox came with the discovery that peroxiredoxin 4 (Prx4) can promote *de novo* disulfide bond formation by utilizing hydrogen peroxide (13, 14). Furthermore, it has been recently revealed

* This work was supported by Grant-in-aid for Scientific Research (S) 24227009 and a grant from the Human Frontier Science Program (HFSP) (to K. N.), by grants from Telethon (GGP11077) and the Associazione Italiana Ricerca Cancro (AIRC; IG and 5 x 1000 program) (to R. S.), and by Japan Society for the Promotion of Science (JSPS) Fellowships 08J03849 and 12J02049) (to K. A.) and 12J04142 (to T. K.).
⌘ *Author's Choice*—Final version full access.
[S] This article contains supplemental Figs. 1–5.
[1] Both authors contributed equally to this work.
[2] Both authors contributed equally to this work.
[3] To whom correspondence may be addressed. Tel.: 39-02-2643-4722; Fax: 39-02-2643-4723; E-mail: sitia.roberto@hsr.it.
[4] To whom correspondence may be addressed. Tel.: 81-75-705-3090; Fax: 81-75-705-3121; E-mail: nagata@cc.kyoto-su.ac.jp.
[5] The abbreviations used are: ER, endoplasmic reticulum; ERGIC, ER-Golgi intermediate compartment; Ero1, ER oxidoreductin-1; ESC, early secretory compartment; PDI, protein disulfide isomerase; Prx4, peroxiredoxin 4; roGFP, redox-sensitive green fluorescent protein; LC-MS/MS, liquid chromatography-tandem mass spectrometry.

that mice with double knock-out of both oxidases exhibit lower birth rate and scurvy, whereas mice with single knock-out (Ero1 or Prx4) exhibit modest effect, indicating mutual complementarity between Ero1 and Prx4 (15). Surprisingly, however, neither Prx4 nor Ero1 contains known ER retention signals (supplemental Fig. 1). Ero1α interacts with PDI and ERp44 (16) and to a minor extent with other family members, including ERp57, ERp46, ERp18, P5, and ERp72 (17–19) In line with their preferential binding, ERp44 and PDI can efficiently retain overexpressed Ero1α (20). On the other hand, it has been unclear how Prx4 is retained in the ER (21).

In this study, we investigated the mechanisms that control the intracellular localization of Prx4. Our findings reveal that Prx4 shares a similar stepwise retention mechanism with Ero1α, in which ERp44 functions as a backup for PDI; when PDI is down-regulated, Ero1α and Prx4 are retained by ERp44 in the downstream compartment of the ER. Such dynamic regulation of two main ER oxidases seems important for maintaining redox homeostasis in the ESC because the expression of Ero1α and Prx4 endowed with KDEL motifs caused hyperoxidizing environment in the ER.

EXPERIMENTAL PROCEDURES

Cells and Antibodies—HeLa and HEK293 cells were cultured in Dulbecco's modified Eagle's medium with 10% fetal bovine serum and antibiotics. The primary antibodies used in the experiments were: mouse monoclonal anti-GFP (Roche Applied Science, Basel, Switzerland), mouse monoclonal anti-HA (Cell Signaling Technology), mouse monoclonal and rabbit polyclonal anti-FLAG (Sigma-Aldrich), mouse monoclonal anti-Prx4 (Abcam, Cambridge, UK), mouse monoclonal anti-Ero1α (Abcam for Western blot and Santa Cruz Biotechnology for immunofluorescence), mouse monoclonal anti-β-actin (Millipore), mouse monoclonal anti-ERGIC53 (Enzo Chemical Laboratories), rabbit polyclonal anti-ERp46 (Santa Cruz Biotechnology), chicken polyclonal anti-P5 (Santa Cruz Biotechnology), rabbit polyclonal anti-PDI (StressGen Biotechnologies Corp.), rabbit polyclonal anti-ERp44 (reported by Ronzoni *et al.* (22)), rabbit polyclonal anti-ERp72 (Santa Cruz Biotechnology), and rabbit polyclonal calnexin (Cell Signaling). The secondary antibodies used in the experiments were: HRP-anti-rabbit IgG, HRP-anti-mouse IgG, Alexa Fluor 488 anti-rabbit or -mouse, and Alexa Fluor 546 anti-rabbit or -mouse (Invitrogen).

Construction of Plasmids—Human Prx4, PDI (wild type or AA mutant), or Ero1α (wild type or C94A mutant) cDNA with a FLAG tag or with a FLAG tag and KDEL sequence at the C terminus was generated by PCR from a Matchmaker Pretransformed Human HeLa library (Clontech) and subcloned into pcDNA3.1. The vectors for the expression of HA-ERp44-WT, C29S, and HA-ERp57 were as described previously (9). DsRed2-ER was purchased from Clontech. ERp44 C29A was generated by site-directed mutagenesis: (forward, 5′-GTA AAT TTT ATG CTG ACT GGG CTC GTT TCA GTC AGA TGT TGC-3′; reverse, GCA ACA TCT GAC TGA AAC GAG CCC AGT CAG CAT AAA AAT TTA C-3′). The ER-targeted redox-sensitive GFP iE variant (ERroGFPiE) was generated from ERroGFPiL (kind gift from Prof. Neil J. Bulleid) by site-directed mutagenesis: (forward, 5′-GGA ATA CAA CTA TAA CTG CGA AAG CAA TGT ATA CAT CAC GGC AG-3′; reverse, 5′-CTG CCG TGA TGT ATA CAT TGC TTT CGC AGT TAT AGT TGT ATT CC-3′).

Transfection, Secretion Assay, and Western Blot—Plasmids and siRNAs were transfected using Effectene® (Qiagen) or Lipofectamine RNAiMAX (Invitrogen), respectively, according to the manufacturer's instructions. For secretion assays, cells were incubated in Opti-MEM for an additional 4–6 h. Secreted materials were precipitated with 15% trichloroacetic acid (TCA) or immunoprecipitated with antibodies and then resolved by SDS-PAGE under reducing or nonreducing conditions. For detection of ERroGFPiE, lysates immunoprecipitated with anti-GFP were loaded. Fluorograms or Western blot images were acquired with the ChemiDoc-It imaging system (UVP, Upland, CA) or with the FLA-9000 Starion (Fujifilm Life Science) and quantified with ImageQuant 5.2 as described by Anelli *et al.* (7). Cells were extracted with 1% Nonidet P-40, 150 mM NaCl, 50 mM Tris-HCl (pH 8.0), and 20 mM *N*-ethylmaleimide. The detergent-soluble fractions of cell lysates were analyzed by Western blot.

Oligonucleotides—Stealth™ RNA siRNAs were obtained from Invitrogen. The sequences were as follows: siPDI-1, 5′-AAU GGG AGC CAA CUG UUU GCA GUG A-3′; siPDI-2, 5′-AUA AAG UCC AGC AGG UUC UCC UUG G-3′; siERp44-1, 5′-AUA GAG UAU ACC UAU AUU CAC UGG G-3′; siERp44-2, 5′-UUA AUU GCC GAG CUA CUU CAU UCU G-3′; and siEro1α, 5′-GGG CUU UAU CCA AAG UGU UAC CAU U-3′. Medium GC Stealth™ RNAi duplexes were used as negative controls.

LC-MS/MS Analysis—Immunoprecipitation was coupled with custom-made direct nano-flow liquid chromatography-tandem mass spectrometry system (Tokyo, Japan). FLAG-tagged Prx4 and mutants thereof were expressed in HEK293 cells and immunoprecipitated with anti-FLAG. Immunoprecipitates were eluted with FLAG peptides and digested with Lys-C endopeptidase (*Achromobacter* protease I). Cleaved fragments were directly analyzed by a direct nano-flow liquid chromatography-tandem mass spectrometry (LC-MS/MS) system as described previously (23). Assays were repeated at least four times.

Immunofluorescence—HeLa cells were washed with phosphate-buffered saline (PBS) and fixed with 4% paraformaldehyde for 20 min at room temperature. Cells were permeabilized with 0.2% Triton X-100 in PBS at room temperature for 5 min followed by incubation in 1% normal goat serum and 1% bovine serum albumin for 1 h. Cells were incubated with primary antibodies for 1 h and then with Alexa Fluor-conjugated secondary antibodies (from Invitrogen Molecular Probes) for 1 h, as indicated. Confocal images were obtained using a LSM 700 confocal microscope and analyzed by the Zen 2009 software (Carl Zeiss, Jena, Germany).

Preparation of Human Recombinant Prx4, Ero1α, PDI, and ERp44—Recombinant Ero1α and PDI were described previously (17, 24). Prx4 and ERp44 were expressed in *Escherichia coli* BL21 (DE3) cells (Novagen) by induction with 0.3 mM isopropyl-1-thio-β-D-galactopyranoside at 30 °C for 6 h just after the A_{600} reached 0.6. Harvested cells were sonicated in 20 mM HEPES (pH 7.5) containing 20 mM imidazole and 150 mM NaCl.

The supernatant from cell lysates was loaded onto a HisTrap column (GE Healthcare) equilibrated with cell suspension buffer and eluted with the same buffer containing 0.5 M imidazole. Eluted fractions were loaded onto a HiLoad 16/60 Superdex 200pg isofraction column equilibrated with 20 mM HEPES-NaOH (pH 7.5) containing 150 mM NaCl. Eluted fractions containing oxidoreductases were desalted and loaded onto a Resource Q column (GE Healthcare) equilibrated with 20 mM Tris-HCl (pH 8.0). Fractions were eluted by a linear gradient of NaCl. Purified proteins were concentrated and stored at −80 °C.

Surface Plasmon Resonance (SPR) Measurement—SPR analyses were performed as described previously (17, 24). Briefly, association or dissociation rate constants (k_{on} or k_{off}) to immobilized Ero1α (WT) or Prx4 were determined by SPR measurements on a ProteOn XPR36 protein interaction array system (Bio-Rad). Ero1α (WT)/Prx4 were coupled to the GLC sensor chip (Bio-Rad) through amine coupling chemistry. As a control, one channel was coupled with BSA to exclude background binding. Sensorgrams were recorded simultaneously for several concentrations (0.444–36 μM, in a 3-fold dilution series) of purified oxidoreductases at 25 °C for a 2-min association phase followed by a 10-min dissociation phase with 20 mM HEPES-NaOH (pH 7.4 or pH 6.4), 150 mM NaCl, 0.001% Tween, and 2 mM EDTA as running and sample buffer. Sensorgrams were analyzed by nonlinear regression analysis according to a two-state model by the ProteOn Manager version 3.0 software (Bio-Rad). Experiments were replicated at least three times.

Statistical Analysis—All data are presented as the means ± S.E. Statistical significance of the difference between groups was evaluated using Student's *t* test. $p < 0.05$ was considered significant. *, $p < 0.05$, **, $p < 0.01$, ***, $p < 0.001$.

Homologous Gene Analysis—To gain an evolutionary perspective, we searched and statistically analyzed homologous genes of ER oxidoreductases using the Kyoto Encyclopedia of Genes and Genomes (KEGG) database (25). The National Center for Biotechnology Information (NCBI) database was also searched for analysis of several sequences (www.ncbi.nlm.nih.gov/protein/).

RESULTS

Interactions of Prx4 and Ero1α with PDI Family Proteins—The ER oxidases Ero1α and Prx4 have at least two common features; one is their function in oxidative protein folding, and the other is their lack of intrinsic ER retention signals. Surprisingly, the latter feature is 100% conserved among Ero1α orthologs and 94.4% conserved among Prx4 in vertebrates (KEGG database (25)) (supplemental Fig. 1). To identify proteins involved in its subcellular localization, we performed LC-MS/MS analyses of the material co-immunoprecipitated with FLAG-tagged Prx4 and identified ERp44, PDI, ERp72, ERp46, and P5 (supplemental Fig. 2) (see also Ref. 18), yielding a pattern similar to what is reported for Ero1α. To further compare the interactomes of the two enzymes and provide additional specificity controls, we overexpressed Prx4-FLAG or Ero1α-FLAG in HeLa cells and analyzed the immunoprecipitates obtained with or without prior cross-linking with dithiobis succinimidyl propionate. Western blot analyses of the material specifically eluted with FLAG peptides confirmed that both Prx4 and Ero1α interact with ERp44, PDI, ERp72, P5, and ERp46 (Fig. 1*A*). The similar binding patterns are in line with coordinated roles of Prx4 and Ero1α in oxidative protein folding (26).

To confirm that endogenous ERp44 and Prx4 interact in physiological conditions, we analyzed Ig-λ producing J558L murine myeloma cells or a transfectant secreting IgM (J[μ_s] (27)). Clearly, endogenous Prx4 can be co-immunoprecipitated with ERp44 in Ig-secreting cells (Fig. 1*B*).

Next, we investigated whether Ero1α and Prx4 co-localize with ERp44 or PDI by immunofluorescence (Fig. 1*C*). Although PDI is primarily localized in the ER, endogenous ERp44 recycles between the ER and cis Golgi and accumulates preferentially in the ERGIC (6, 7). Consistent with the results shown in Fig. 1*A*, both Ero1α and Prx4 showed co-localization with PDI and ERp44 in HeLa cells (Fig. 1*C*). Co-localization was stronger with PDI, suggesting that Ero1α and Prx4 were mainly localized in the ER and to a lesser extent in the ERGIC. In many cells, co-staining with ERp44 and PDI was more evident for Prx4 than Ero1α (data not shown), which may reflect the localization of part of Ero1α in mitochondria-associated ER membranes (28, 29).

Secretion of Overexpressed Prx4 Is Inhibited by ERp44 and PDI—Confirming previous observations (30), overexpressed Prx4 was clearly secreted by HeLa cells (Fig. 2*A*, *lane 2*), implying that saturable mechanisms determine its intracellular retention. Co-expression of ERp44 or PDI, but not of ERp57, restored retention of overexpressed Prx4 (Fig. 2*A*, *lanes 3–5*). These secretory phenotypes were similar for Ero1α (Fig. 2*B*). In the experiment shown, ERp57 partly inhibited secretion of overexpressed Ero1α, albeit much less efficiently than ERp44 or PDI (Fig. 2*B*, *lane 5*) (20). ERp57 cooperates with calnexin and calreticulin to promote glycoprotein folding. The absence of glycosylation sites in Prx4 may explain why co-expressed ERp57 did not affect its secretion. Thus, ERp44 and PDI but not ERp57 can retain overexpressed Prx4.

In thiol-dependent quality control, Cys-29 in the atypical redox-active motif of ERp44 forms mixed disulfides with Ero1 and client proteins such as IgM, adiponectin, or SUMF1/FGE (sulfatase-modifying factor 1/formylglycine-generating enzyme) (5). Clearly, Prx4-FLAG secretion was decreased in a dose-dependent manner by wild type HA-ERp44 (WT) but not by a mutant in which Cys-29 was replaced by a serine (yielding ERp44 C29S, Fig. 2*C*). In contrast, a PDI mutant in which cysteine residues of the two *CXXC* motifs were replaced by alanine residues (PDI-AA) inhibited Prx4 secretion almost as efficiently as wild type molecules (Fig. 2*D*). Thus, the enzymatically active cysteine residues of PDI are not necessary for retention of Prx4.

Because Prx4 shares similar retention mechanisms with Ero1α, the two proteins could compete with each other. Accordingly, secretion of Prx4-FLAG was dramatically increased by Ero1α-FLAG co-expression (Fig. 2*E*, compare *lanes 2* and *4*). Also an enzymatically inactive mutant of Ero1α (Ero1α-C94A) promoted Prx4 secretion (Fig. 2*E*, *lane 5*). Conversely, secretion of Ero1α-FLAG was not increased by co-expression of abundant Prx4-FLAG (Fig. 2*F*, *lanes 2* and *4*).

PDI Preferentially Retains Ero1α, whereas ERp44 Equally Retains Ero1α and Prx4—The unidirectional competition between Ero1α and Prx4 suggested that the former binds to its retainers more efficiently than the latter. Therefore, we ana-